PGC PUBLISHING

McInnes, B.I.A., Evans, N.J., Fu, F.Q., Garwin, S., Belousova, E., Griffin, W.L., Bertens, A., Sukarna, D., Permanadewi, S., Andrew, R.L., Deckart, K., 2005 - Thermal History Analysis of Selected Chilean, Indonesian and Iranian Porphyry Cu-Mo-Au Deposits; *in Porter, T.M. (Ed.), Super Porphyry Copper & Gold Deposits: A Global Perspective*; PGC Publishing, Adelaide, v. 1, pp 27-42.

THERMAL HISTORY ANALYSIS OF SELECTED CHILEAN, INDONESIAN AND IRANIAN PORPHYRY Cu-Mo-Au DEPOSITS

[1]Brent I.A. McInnes, [1]Noreen J. Evans, [2]Frank Q. Fu, [3,4]Steve Garwin, [5]Elena Belousova, [1,5]W.L. Griffin, [6]Alfredo Bertens, [7]Djadjang Sukarna, [7]Sam Permanadewi, [8]Ross L. Andrew and [9]Katja Deckart

[1]*CSIRO Exploration and Mining, Bentley, WA, Australia*
[2]*School of Geosciences, University of Sydney, NSW Australia*
[3]*Centre for Exploration Targetting, University of WA, Perth, Australia*
[4]*Geoinformatics Exploration Australia, West Perth, Australia*
[5]*GEMOC Key Centre, Macquarie University, NSW, Australia*
[6]*CODELCO-Chile, Santiago, Chile*
[7]*Geological Research and Development Centre, Bandung, Indonesia*
[8]*Rio Tinto Exploration Pty. Limited, Bundoora, Victoria Australia,*
[9]*Departamento de Geología, Universidad de Chile, Santiago, Chile.*

Abstract - This paper presents U-Pb-He triple-dating age determinations for several porphyry Cu±Mo±Au deposits in Chile, Indonesia and Iran in an effort to determine their thermal histories and to explore the effects of cooling/exhumation rates on ore formation and preservation processes. Inverse thermal modelling of measured time-temperature history data from these deposits was conducted to quantitatively constrain the depth of emplacement, duration of ore deposition, exposure ages and cooling/exhumation rates. The duration of hypogene ore formation for the deposits studied generally occurs within timeframes of 10^5 years, although modelling results for the Grasberg, Batu Hijau and El Teniente super porphyry deposits suggest formation periods of the order of 10^4 years. Emplacement depths on intrusions associated with porphyry mineralisation range from 800 m to 5500 m from the palaeosurface, with Grasberg and Rio Blanco being respectively the shallowest and deepest super porphyry deposits studied. The thermochronology data indicates a positive correlation between metal grade and cooling rate during hypogene ore formation, but further investigation is warranted. Exhumation rates varying from 0.3 to 1.1 km/m.y. have implications for the preservation potential of hypogene ore deposits, with super porphyry deposits like Sar Cheshmeh potentially losing 3.5 Mt of copper to erosion over the last 5 million years. The potential for supergene ore formation under such conditions is high, as is the potential for the formation of proximal Exotica-type deposits.

Introduction

Helium (^{4}He), in addition to the radiogenic isotopes of Pb, is a natural fission product of the U and Th decay series. Similar to the U-Pb geochronology system, age relationships in the (U-Th)/He system can be determined by measuring the concentrations of both the parent (^{235}U, ^{238}U and ^{232}Th) and daughter (^{4}He) isotopes in minerals. In contrast to Pb, He diffuses through the mineral lattice more readily and at lower temperatures, a characteristic that Zeitler *et al.*, (1987) predicted could have potential applications in low temperature thermochronology. Quantitative He diffusion measurements in minerals (Farley, 2002 and references therein) provided the necessary parameters required for determining the thermal history of the Earth's crust, and have led to the development of new applications for (U-Th)/He dating in economic geology research (McInnes *et al.*, 1999; Arehart *et al.*, 2003; Evans *et al.*, in press).

Despite the fact that porphyry deposits have been exploited for 100 years (open pit mining at Bingham began in 1905), a number of time- and temperature-related variables involved in their genesis remain poorly understood:

i) depth of emplacement,
ii) longevity of the ore precipitation event during the thermal decline of the magmatic-hydrothermal system,
iii) preservation potential of hypogene ores during orogenic uplift and exhumation, and
iv) formation potential of supergene ores from eroded hypogene precursors.

Thermochronology techniques that can address these issues have significance for ore genesis studies and mineral exploration. The (U-Th)/He method is particularly amenable to application in porphyry deposit research because many of the minerals suited to dating occur as accessory phases in porphyritic intrusions known to host disseminated mineralisation. Diffusion experiments on fluorite, apatite, titanite, zircon and rutile have determined a progressive increase in minimum He closure temperature

(T_c) from ~60°C to ~200°C (Farley, 2002; Reiners *et al.*, 2002; Crowhurst *et al.*, 2002; Evans *et al.*, in press). Therefore, (U-Th)/He dating is most commonly used as a *thermochronometer* to determine cooling ages and not as a *geochronometer* to determine formation ages (eg., U-Pb). However, by combining U-Pb (T >900°C; Lee *et al.*, 1997; Cherniak and Watson, 2000), K-Ar, Re-Os (T range from 300-500°C; McDougall and Harrison, 1999; Suzuki *et al.*, 1996), fission track (eg. Arehart *et al.*, 2003; apatite fission tracks anneal at ~125°C) and (U-Th)/He techniques, an interval of over 800°C of thermal history of an ore deposit or mineral district can be elucidated.

In this paper we report the results of combining a number of these conventional thermochronology techniques with the (U-Th)/He method. Our preferred approach for determining the thermal histories of porphyry deposits involves combining zircon U-Pb, zircon (U-Th)/He and apatite (U-Th)/He dating methods on the same sample of rock. The advantages of this U-Pb-He "triple-dating" approach are that:

i) *A single radioactive decay scheme is utilised U + Th - Pb + He,*
ii) Apatite and zircon are both usually obtainable in significant quantities for analysis from a 1 kg sample of igneous rock,
iii) Apatite and zircon are stable in potassic, phyllic and propylitic alteration assemblages in porphyry deposits,
iv) The coupled use of zircon U-Pb and zircon (U-Th)/He dating determines both the emplacement age of the porphyry deposit and the interval where the bulk of base metal transport and deposition occurs in magmatic-hydrothermal systems (750-200°C),
v) The coupled use of zircon (U-Th)/He and apatite (U-Th)/He dating determines the post-mineralisation uplift and exhumation history of the deposit with implications for ore preservation and supergene remobilisation (200-90°C).

Methods

U-Pb-He triple-dating was conducted on rock samples from selected porphyry deposits in Cu±Mo±Au metallogenic belts in Chile, Indonesia and Iran using the analytical methods described below. This data was combined with previously published geochronology results for comparison purposes and, where possible, to establish complete thermal histories of the deposit using an inverse thermal modelling approach.

U-Pb and (U-Th)/He Analytical Procedures

Apatite and zircon grains for (U-Th)/He thermochronology were selected by hand picking in order to avoid U- and Th-rich mineral inclusions that may contribute excess helium. Images of selected grains were recorded digitally and grain measurements were taken for the calculation of an alpha correction factor (Farley *et al.*, 1996). Helium was thermally extracted from single crystals that were loaded into platinum micro-crucibles and heated using a 1064 nm Nd-YAG laser. ^{4}He abundances were determined by isotope dilution using a pure ^{3}He spike, calibrated daily against an independent ^{4}He standard tank. The uncertainty in the sample ^{4}He measurement is <1%. The U and Th content of degassed apatite is determined by isotope dilution using ^{235}U and ^{230}Th spikes. Apatite is digested in 7M HNO_3 and zircon is digested in Parr bombs using HF. Standard solutions containing the same spike amounts as samples were treated identically as were a series of unspiked reagent blanks. For single crystals digested in small volumes (0.3-0.5 ml), U and Th isotope ratios were measured to a precision of <3%. Overall the (U-Th)/He thermochronology method at CSIRO has a precision of 2.5% for apatite, based on multiple age determinations (n=70) of Durango standard which produce an average age of 31.5±1.6 (2σ) Ma.

Zircon U-Pb dating at Macquarie University utilises a LA-ICP-MS facility combining a New Wave/Merchantek 213 nm UV laser ablation (LA) system and a HP 4500 ICP-MS, with analytical methods detailed by Jackson *et al.* (2004). A split sample of zircon grains from the (U-Th)/He study was mounted in epoxy discs and polished to expose the grains. The mounts were examined using back-scattered electron/cathodoluminescence microprobe imaging to record internal zonation features and external morphology prior to selecting grains for analysis. U-Pb geochronology results were based on the analysis of ^{207}Pb/^{235}U, of ^{208}Pb/^{232}Th, and ^{206}Pb/^{238}U on between 14 and 20 grains per sample. The analysis of the sample zircons was bracketed by multiple analyses of the gem quality GJ-1 zircon, and other in-house standards 91500 and Mud Tank zircon (Wiedenbeck *et al.*, 1995; Black and Gulson, 1978) were analysed in every run as an independent control on reproducibility and instrument stability.

Graphical Interpretation and Inverse Modelling of Thermal Histories

The data outputs from mineral chronometry are radiometric ages tied to nominal closure temperatures. Multiple age determinations produce time-temperature curves delineating the thermal history of a porphyry deposit from the time of its emplacement to the time of its thermal decline to ambient conditions. Graphical analysis of combined age-temperature data shows a range of cooling profiles varying from a sub-vertical line for a rapidly cooled intrusion emplaced in the upper 1-2 km of the crust (see right inset in Fig. 1) to a "hockey stick" pattern for a slowly cooled pluton emplaced at depths greater than 2-3 km in the crust (see left inset in Fig. 1). Using the "hockey stick" as a process model for the thermal histories of porphyry copper systems, the handle of the stick (represented by higher temperature chronometers like zircon U-Pb and K-Ar) constrains the high-temperature history of the pluton and its associated Cu ore shell, while the blade of the stick (zircon (U-Th)/He and apatite (U-Th)/He chronometers) constrain the post-mineralisation uplift and exhumation history of the deposit with implications for ore preservation and supergene remobilisation.

The graphical interpretation can be further refined using a computational approach where the raw time-temperature data is input into an "inverse modelling" algorithm that quantifies a number of parameters related to the dynamic

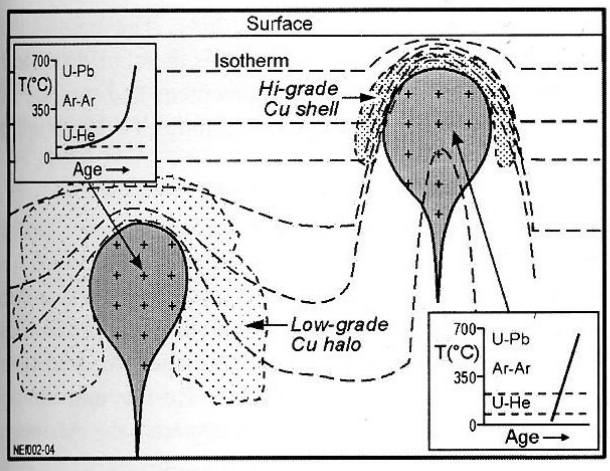

Figure 1: ***A schematic representation of pluton emplacement at shallow (right) and deep (left) crustal levels and the respective time-temperature histories*** *(insets).* If Cu transport and heat transfer are treated as diffusive processes, then intrusions emplaced within the uppermost crust should experience greater thermal gradients and more effective Cu transport than those emplaced in mid-crustal regions where temperature regimes are moderated by the Earth's geotherm.

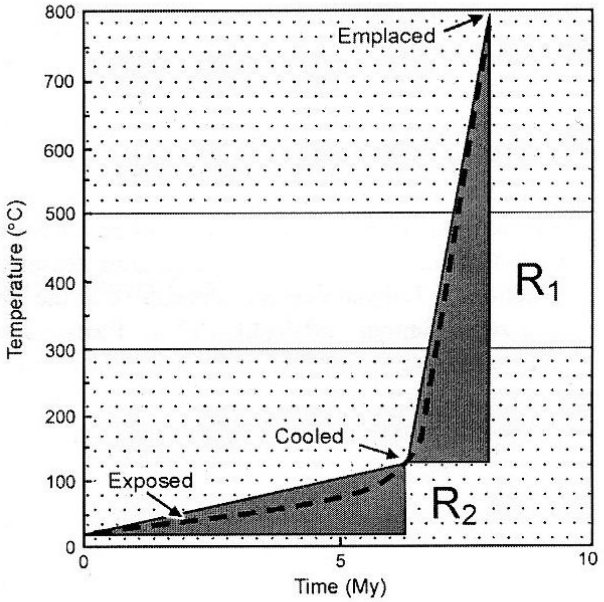

Figure 2: ***Schematic time-temperature plot showing rates of magmatic-hydrothermal cooling (R_1) and exhumation cooling (R_2).***

processes of magmatic-hydrothermal cooling, exhumation and erosion of igneous intrusions (Fu *et al.,* 2005). An inverse thermal modelling software package, GeoModel v. 1.0, has been developed by Frank Fu as part of his PhD study at University of Sydney. Physical parameters and assumed initial conditions for porphyry deposits discussed in this paper are listed in Table1 and background information on modelling techniques is provided in Appendix 1. The current version of GeoModel inverts thermochronology data assuming conductive heat transfer, which is the least efficient heat transfer mechanism and therefore, the outputs of the modelling runs provided in this paper should be considered as end members. For example, if the depth of porphyry emplacement is constrained by the model to be 5 km, then that result is a minimum depth. Future versions of GeoModel will include advective and convective cooling scenarios, although our approach in this paper is to compare and contrast a number of porphyry deposits assuming the same initial conditions so that relative depths of emplacement can be determined.

GeoModel v. 1.0 treats the cooling history of igneous bodies from their assumed emplacement temperature at 1000°C to an ambient surface temperature of 10°C. Throughout the cooling history, two distinct phases have been defined: i) *Magmatic-hydrothermal cooling* begins at intrusion emplacement and continues until both igneous and country rocks reach a final thermal equilibrium under a steady-state geothermal gradient. This phase is shown as R_1 on the schematic time-temperature plot (Fig. 2). Initial cooling is rapid, but towards the end of the magmatic-hydrothermal cooling stage, the igneous and country rocks cool more slowly until both reach a final thermal equilibration and the geothermal gradient returns to pre-intrusion thermal conditions (defined as the "cooled" state), ii) *Exhumation cooling* (R_2 in Fig. 2) begins when the intrusion reaches the "cooled" state and continues until the body reaches the surface (at 10°C). The rate of cooling through this stage is primarily controlled by exhumation and erosion processes. The hypogene deposition of most economic minerals (e.g. Cu, Au) mainly occurs during the early magmatic-hydrothermal cooling stage while supergene remobilisation and precipitation processes occur mainly during the late exhumation cooling stage.

Parameter	Initial Value
Surface temperature	10 °C
Geothermal gradient	50 °C/km
Initial temperature of magma	1000 °C
Thermal diffusivity	1.0×10^{-6} m²/s
Latent heat of crystallisation	100 cal/g
Constant heat flow from bottom	65 mW/m°C

Table 1: ***Main parameters and their initial values used in the modelling*** (Fu *et al.,* 2005).

The following sections review previous work on selected porphyry deposits in Iran, Indonesia and Chile (Figs. 3 to 8) and present new geo- and thermochronometry data (Table 2). The measured geochronology data was input into GeoModel v. 1.0 and iterations were performed to yield an idealised cooling history that successfully passed through all the age data (see Appendix 1). The GeoModel v. 1.0 outputs (Table 3) were used to determine the duration of the Cu deposition interval (arbitrarily defined as 500 to 300°C), the depth of emplacement of the intrusion and the average exhumation rate of the crustal block hosting the intrusion thereby indicating the preservation potential of satellite hypogene deposits and an estimate of the amount of hypogene ore eroded.

Porphyry Deposits of the Kerman Belt, Iran

The Kerman Belt, located in southeastern Iran, is a NNW-SSE elongated mountain belt 500 km long and 100 km wide. It is principally composed of a folded and faulted early Tertiary volcano-sedimentary complex and is bordered to the southwest by a major thrust zone and the

Tertiary and Palaeozoic sedimentary rocks of the Zagros Mountains (Waterman and Hamilton, 1975). The Sar Cheshmeh and Meiduk copper deposits are two of the largest known porphyry Cu systems in the Kerman district. Both deposits are currently being mined by the National Iranian Copper Industries Company (NICICO). Sar Cheshmeh and Meiduk are associated with an Eocene high-K calc-alkaline volcanic arc formed after cessation of subduction of Tethyan oceanic lithosphere at the Zagros suture zone (Sengor and Kidd, 1979). Post-collisional compression and mantle buoyancy forces led to the uplift of the Iranian plateau, with middle Miocene marine sediments occurring at elevations greater than 3000 m in the Kerman belt (Hassanzadeh, 1993). The preservation of porphyry Cu deposits in the belt is therefore dependent on the original depth of emplacement and the rate of exhumation in response to this tectonically driven uplift and erosion.

No previous thermochronometry studies have been carried out in the Kerman District. In this study we have determined the zircon U-Pb, zircon (U-Th)/He and apatite (U-Th)/He ages of igneous units from the potassic alteration zone of several porphyry Cu systems, and integrated these data with pre-existing Rb-Sr, Re-Os and Ar-Ar geochronology ages. These ages constrain the maximum

Deposit/Location	Age (Ma) ±2σ	Method
SCP Sar Cheshmeh, Iran	13.6 ± 0.1	Zircon U-Pb[1]
	12.2 ± 1.2	Rb-Sr (3-point isochron)[2]
	12.5 ± 0.5[2]	Biotite K-Ar
	10.9 ± 0.1	Zircon U-He[1]
	7.2 ± 0.4	Apatite U-He[1]
Meiduk, Iran	12.5 ± 0.1	Zircon U-Pb[1]
	12.4 ± 0.5	Rb-Sr (3 point isochron)[3]
	11.2 ± 0.5	Biotite Ar-Ar[3]
	10.8 ± 0.4	Sericite Ar-Ar[3]
	12.5 ± 0.5	Zircon U-He[1]
	9.5	Apatite U-He*
Adbar, Kuh-eMasahim, Iran[4]	7.5 ± 0.1	Zircon U-Pb[1]
	6.8 ± 0.4	Biotite Ar-Ar[5]
	6.4 ± 0.8; 6.3 ± 0.9	Hornblende Ar-Ar[5]
	7.3 ± 0.3	Zircon U-He[1]
	4.9 ± 0.4	Apatite U-He[1]
Grasberg, Indonesia	2.9 ± 0.3	Re-Os[6]
	3.33 ± 0.12; 3.01 ± 0.06	Biotite Ar-Ar[7]
	3.1-2.9 ± 0.1	Apatite U-He[1]
Batu Hijau, Indonesia Young Tonalite	3.74 ± 0.14	Zircon U-Pb[8]
	3.73 ± 0.08	Biotite Ar-Ar[8]
	2.23 ± 0.09	Apatite U-He[1]
Ciemas, Indonesia	17.8 ± 0.4	Zircon U-Pb [1]
	16.8 ± 0.1	Hornblende K-Ar[9]
	15.2 ± 2.7	Sulphide Re-Os[10]
	7.2 ± 0.24	Apatite U-He[1]
[11]Rio Blanco, PDL, Chile	5.23 ± 0.07	Zircon U-Pb[11]
	3.9 ± 0.09	Zircon U-He[1]
	2.4 ± 0.1	Apatite U-He[1]
[11]Rio Blanco, PQM, Chile	6.32 ± 0.06	Zircon U-Pb[11]
	4.95 ± 0.18	Zircon U-He
	3.5 ± 0.14	Apatite U-He
[1] El Teniente, Chile (Teniente dacite)	5.05 ± 0.12	Zircon U-Pb
	5.14 ± 0.03	Re-Os (moly)
	4.96 ± 0.03	Ar-Ar
	2.74 ± 0.3	Apatite U-He

*No apatite was recovered from the Meiduk samples. As Abdar is located only 18 km away and the erosion rate in the area is thought to be similar on this geographic scale, the difference between the zircon and apatite (U-Th)/He ages at Abdar was applied to Meiduk resulting in a proxy apatite (U-Th)/He age of 9.5Ma. [1]This work; [2]Shahabpour, 1982; [3]Hassanzadeh, 1993; [4]Abdar diorite subvolcanic intrusion in caldera of Kuh-e-Masahim volcano; [5]Hassanzadeh, 1993, lava flows on flanks of Kuh-e-Masahim volcano; [6]Mathur *et al.*, 2000b; [7]Pollard *et al.*, 2004; [8]Garwin, 2000; [9]Cartwright, 1998; [10]McInnes *et al.*, 2000; [11]Deckart *et al.*, 2005. All errors 2σ;

Table 2: ***Age data for the selected Iranian, Indonesian and Chilean porphyry deposits***

period of longevity of potential hydrothermal mineralisation in porphyry-epithermal environments. The thermal histories for Sar Cheshmeh and Meiduk are compared to that of the Abdar Cu-Au prospect hosted within the collapsed and partially eroded caldera of the Kuh-e-Masahim stratovolcano located between the two porphyry copper deposits.

Sar Cheshmeh Porphyry Cu Deposit

The Sar Cheshmeh Cu deposit (1100 Mt @ 0.64% Cu, 0.03% Mo) is located on the northeastern slopes of Kuh-e-Mamzar, about 60 km south-southwest of Rafsanjan. The ore body is contained within an ovoid (2.5 x 1 km) Cu shell surrounding a Cu-poor granodiorite to quartz monzonite intrusion known as the Sar Cheshmeh porphyry (SCP) that was emplaced within Eocene to Oligocene volcanic rocks of andesitic composition (Fig. 1). The alteration halo and satellite intrusions extend for 7 km.

During Cu ore formation, the deposit was intruded by 3 igneous units interpreted by Ghorashi-Zadeh (1979) to be fractional crystallisation products of the same magma chamber that produced the SCP. Cross-cutting relationships define the order of emplacement of the intramineral intrusions as: i) late fine porphyry (fine-grained quartz monzonite); ii) early hornblende porphyry (dacite); and iii) late hornblende porphyry (latite dyke swarms). Although these intrusions played a role in redistributing Cu throughout the deposit, their net contribution to ore genesis has been to dilute the initial Cu content of the Sar Cheshmeh porphyry. Shahabpour (1982) determined Rb-Sr and K-Ar ages for the Sar Cheshmeh porphyry (12.2 ± 1.2 Ma and 12.5 ± 0.5 Ma, respectively; Table 2). In this work, zircon U-Pb/(U-Th)/He and apatite (U-Th)/He dating was conducted on samples of the SCP obtained from the open pit in August 2002.

Meiduk Porphyry Cu Deposit

The Meiduk Cu deposit (>170 Mt @ 0.82% Cu) is associated with a 700 x 400 m quartz diorite stock known as the Meiduk porphyry (Fig. 2). The intrusion hosts 90% of the Cu mineralisation and is cross-cut by multiple NNE trending dykes called the Meiduk fine porphyry. The dykes are of similar composition to the main intrusion and are interpreted as comagmatic (Hassanzadeh, 1993).

The age data for the Meiduk porphyry are presented in Table 2. Zircon U-Pb and zircon (U-Th)/He ages of 12.5 Ma for the Meiduk porphyry are essentially identical to mineral-whole rock Rb-Sr ages (12.4 ± 0.5 Ma) reported by Hassanzadeh (1993). That study also determined Ar-Ar isochron ages of 11.2 ± 0.5 Ma for biotite in potassic alteration assemblages and 10.8 ± 0.4 Ma for sericite in phyllic alteration zones. Similar to Sar Cheshmeh, the progressively decreasing ages for the Meiduk porphyry in the U-Pb and Ar-Ar systems reflects the cooling history of the deposit through the temperature interval 750°C to 300-350°C, yielding a cooling rate of 250-350°C/m.y.

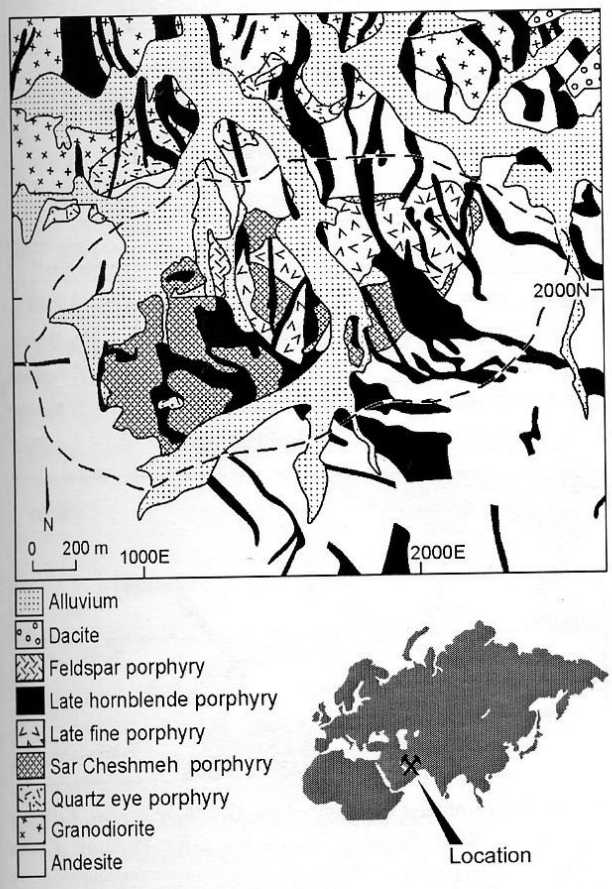

Figure 3: ***Geology of the Sar Cheshmeh Cu-Mo deposit*** (modified from Ghorashi-Zadeh, 1979; Waterman and Hamilton, 1975). Mineralisation is associated with the granodiorite stock intruded into folded and faulted early Tertiary volcano-sedimentary sequences. Dashed line = open pit boundary.

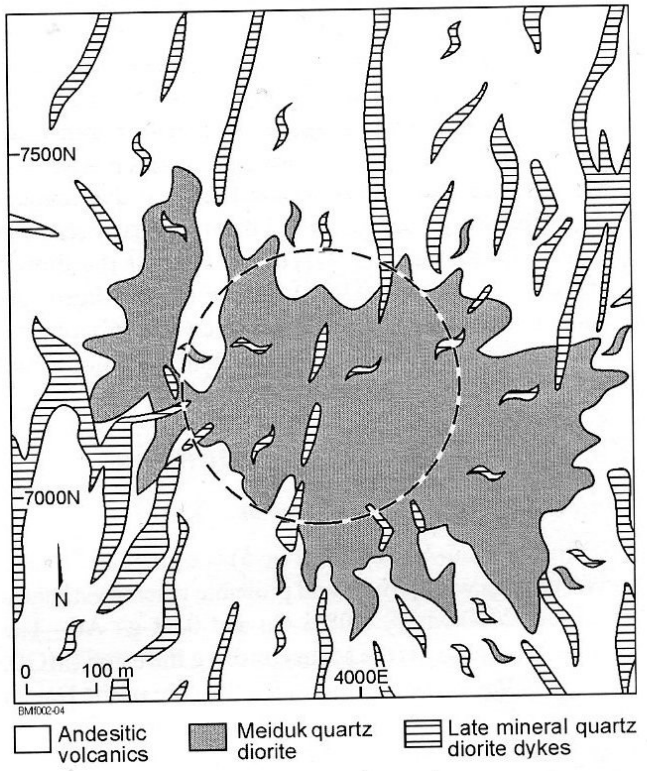

Figure 4: ***Simplified geology of the open pit area at the Meiduk porphyry Cu deposit, Iran*** (modified from Meiduk mine geology report). The deposit lies within a basin on the Kuh e La Chah (La Chah Mountain), about 45 km from Shahr e Babak. The porphyry complex consists of multiple intrusions of mainly quartz diorite composition (Hassanzadeh, 1993). Dashed line = approximate ore limit. Meiduk is 85 km SSW of Sar Cheshmeh (see Fig. 3 for location).

Surprisingly, the zircon (U-Th)/He age is identical to the zircon U-Pb age for the same sample of Meiduk porphyry, implying that either: i) the Meiduk sample from this study has been emplaced near a contact with cool country rock and therefore has had a more rapid cooling history than the samples in the Ar-Ar study, or ii) that zircon (U-Th)/He in rapidly cooled, high level intrusions acts as a *geo*chronometer, rather than a *thermo*chronometer. No apatite was recovered from the Meiduk samples and in order to facilitate modelling, a value of 9.5 Ma was assigned as the apatite (U-Th)/He age. As Abdar is located only 18 km away, and the erosion rate in the area is thought to be similar to that at Mikuk, the difference between the zircon and apatite (U-Th)/He ages at Abdar was subtracted from the zircon (U-Th)/He age for Meiduk resulting in a proxy apatite (U-Th)/He age of 9.5Ma.

Abdar Cu-Au Prospect, Kuh-e-Masahim Volcano

The Abdar Cu-Au prospect, located approximately 15 km southeast of Meiduk, is associated with a subvolcanic dioritic intrusion hosted within the partially eroded caldera of the Kuh-e-Masahim stratovolcano (35 km basal diameter, 3500 m asl total elevation, 1500 m elevation above surrounding plateau). Epithermal high-sulphidation Au-Ag-base metal veins were exposed in the caldera peripheral to the Abdar Cu prospect. Reconnaissance scale drilling of the prospect has detected anomalous yet uneconomic concentrations of Cu (values ranging from 0.1-0.25% Cu). Samples for geochronology investigation were taken from potassic alteration zones from mineralised drill core. Similar to Meiduk, the zircon U-Pb and zircon (U-Th)/He age data for the Abdar diorite (Table 2) are identical within error. This further supports the suggestion that the zircon (U-Th)/He system acts as a *geo*chronometer for shallow, rapidly cooled subvolcanic intrusions. The relatively young Ar-Ar ages for lava flows on the flanks of the volcano indicate that the feeder conduits did not thermally reset the zircon U-Pb and zircon (U-Th)/He ages of the diorite intrusion. The apatite (U-Th)/He age of 4.9 Ma for the Abdar diorite indicates the time when the subvolcanic intrusion cooled below 90°C due to caldera collapse and rapid erosion of the overlying volcanic pile.

Porphyry Deposits in Indonesia

Grasberg Porphyry Cu-Au Deposit

The Grasberg Cu-Au deposit (Fig. 5) is a giant ore system in West Papua with proven and probable reserve estimates of around 2700 Mt @ 1.08% Cu and 0.98 g/t Au. The economic porphyry is the Main Grasberg Intrusion (MGI), a quartz monzodiorite that intruded the core of the Dalam Diatreme. The final stage of magmatic activity at Grasberg was the emplacement of the dyke-like Kali intrusion. Although zircon U-Pb dating has not yet been carried out, combined Ar-Ar and (U-Th/He) dating on the same samples from the MGI and Kali intrusions shows extremely rapid cooling with apatite (U-Th)/He ages (2.9 to 3.1 [± 0.1] Ma); McInnes *et al.*, 2004) nearly identical to biotite $^{40}Ar/^{39}Ar$ ages (from 3.0 to 3.3 [± 0.1] Ma; Pollard *et al.*, 2004). These ages overlap with a sulphide Re-Os age of 2.9 ± 0.3 Ma (Mathur *et al.*, 2000a) indicating that ore-related intrusions in the district underwent extremely rapid cooling as a consequence of shallow emplacement, corroborating earlier interpretations based on fission track dating that the MGI was emplaced within ~1 km of the palaeosurface (Weiland and Cloos, 1996).

Batu Hijau Porphyry Cu-Au Deposit

The Batu Hijau porphyry Cu-Au deposit (Fig.6) is located in southwestern Sumbawa Island, Nusa Tenggara with proven and probable reserve estimates of around 920 Mt @ 0.55% Cu and 0.41 g/t Au. Mineralisation is associated with a multi-phase tonalite porphyry complex hosted in quartz-dioritic and andesitic wallrocks. Zircon U-Pb and apatite (U-Th)/He ages (Table 2) for the late-mineralisation Young Tonalite (collected at 150 m A.S.L.) are 3.74 ± 0.1 Ma (Garwin, 2000) and 2.23 ± 0.09 Ma respectively. Hydrothermal biotite from the Young Tonalite (collected from 150-350 m A.S.L.) yields a mean plateau Ar-Ar age

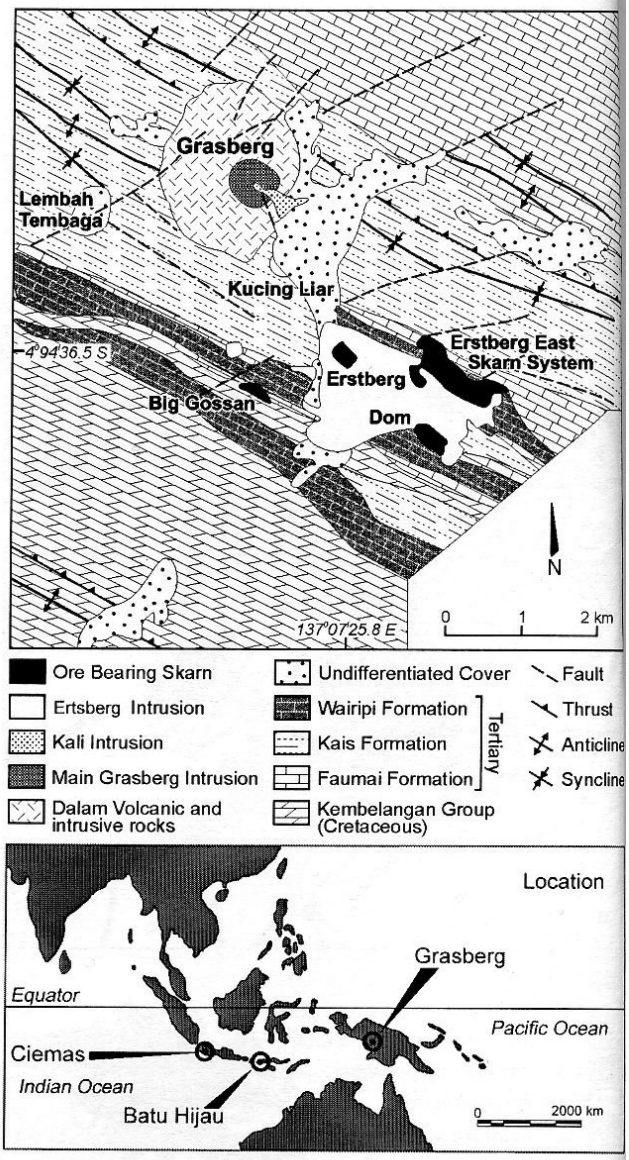

Figure 5: ***Simplified Geology of the Grasberg region, Ertsberg District, West Papua, Indonesia*** (after Pollard). Cu-Au mineralisation is related to Pliocene diorite to quartz monzonite intrusive rocks emplaced in Cretaceous and Tertiary siliciclastics and carbonates. The Grasberg deposit is hosted within the Dalam volcanic and intrusive complex although some mineralisation also occurs along a series of skarns, shown on the plan (Pollard *et al.*, 2004). Lower inset shows the location of Grasberg relative to the other two deposits discussed in Indonesia, Batu Hiujau on Sumbawa Island and Ciemas on Java.

of 3.73 ± 0.08 (2σ) Ma, which is indistinguishable from the zircon U-Pb age. Previous studies using amphibole-plagioclase thermobarometry indicate that the tonalitic magmas began to crystallise at 9 km depth (710-780°C) with final crystallisation occurring at ≤2km (± 0.5km) depth (Garwin, 2000; 2002).

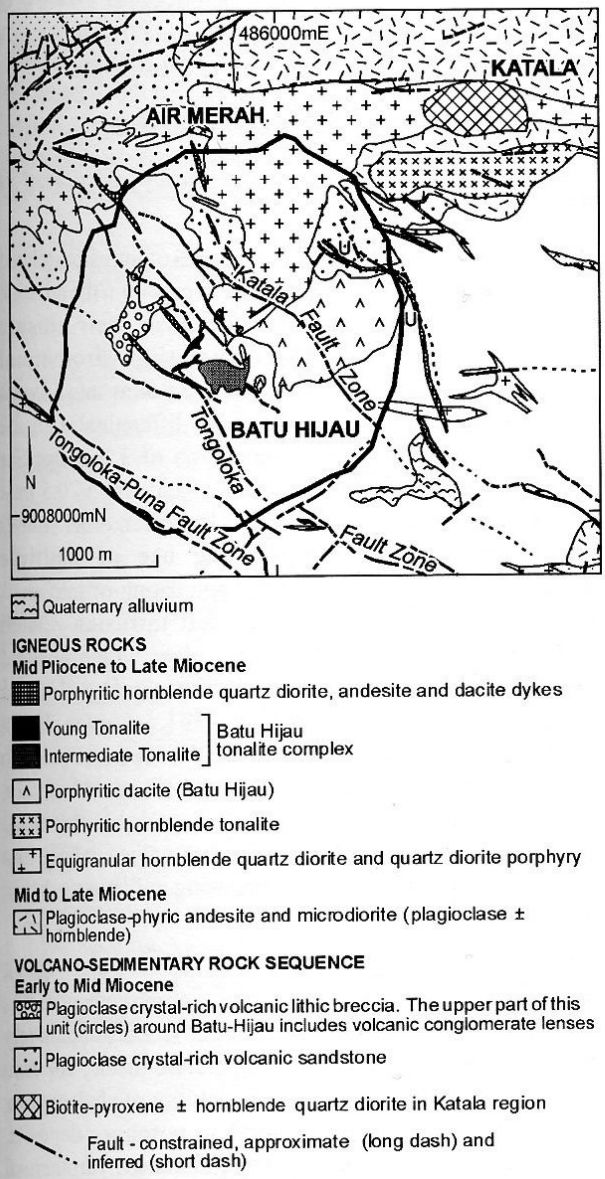

Figure 6: ***Simplified geology of the Batu Hijau Cu-Au district and mine, southwestern Sumbawa, Indonesia*** (after Garwin, 2000). The deposit formed during emplacement of a Neogene tonalitic intrusive complex into older quartz diorite and andesitic volcaniclastics of the Sunda-Banda volcanic island arc (Garwin, 2002). Solid line denotes ultimate pit outline. See Fig. 5 for location.

Ciemas Cu-Au Porphyry Prospect

The Ciemas porphyry Cu-Au prospect is located near the southern coast of western Java, about 150 km south of Jakarta. The prospect has seen limited drilling (<10 diamond holes) and development, but the results to date suggest extensive zones of sub-economic metal grades (~0.2% Cu, ~0.2% Au) associated with a quartz diorite porphyry intrusion hosted principally by andesitic volcanic host rocks. Zircon U-Pb, hornblende K-Ar (Cartwright, 1998), sulphide Re-Os (McInnes *et al.*, 2000) and apatite (U-Th)/He geochronology has returned ages of 17.8, 16.8, 15.2 and 7.2 Ma, respectively (Table 2).

Porphyry Deposits in Chile

Chuquicamata

The thermal history of the Chuquicamata porphyry Cu-Mo deposit of northern Chile has been studied extensively and from various perspectives. Ballard *et al.*, (2001) analysed zircon by excimer laser ablation-inductively coupled plasma-mass spectrometry (ELA-ICP-MS) and by sensitive high-resolution ion microprobe (SHRIMP) to reveal that two temporally distinct magmatic-hydrothermal systems make up the giant Chuquicamata deposit (East Porphyry: 34.6 ± 0.2 Ma; Bench and West Porphyries; 33.3 ± 0.3 Ma and 33.5 ± 0.2 Ma;). The age of the East Porphyry agrees well with a $^{40}Ar/^{39}Ar$ age generated by Reynolds *et al.*, 1998 (34.9 ± 0.3 Ma) and a Re-Os molybdenite age (34.8 ± 0.2 Ma; Mathur *et al.*, 2000a). The geochronology age of the younger Bench and West porphyries correlates with the $^{40}Ar/^{39}Ar$ age (33.4 ± 0.3 Ma) for potassic alteration determined by Reynolds *et al.*, (1998) and agrees within error with the Re-Os isochron for associated pyrite (Mathur *et al.*, 2000a). Given the closure temperature for the various methods, the East, Bench and West porphyries cooled from ≈750°C (zircon crystallisation) to below 300°C (closure temperature for Ar diffusion from biotite) in less than half a million years yielding a magmatic-hydrothermal cooling rate of 1000°C/m.y. (Ballard *et al.*, 2001). Apatite (U-Th)/He ages of around 31 Ma (McInnes *et al.*, 1999) for potassic alteration assemblages in the West porphyry however indicate a total cooling rate of the Chuquicamata ore body of the order of 200-300°C/m.y. Unfortunately, Chuquicamata was not specifically sampled for triple-dating as part of this study. With a complete suite of samples with well-documented positions, age data can be analysed and more definitive cooling rates provided for both the East and West porphyries.

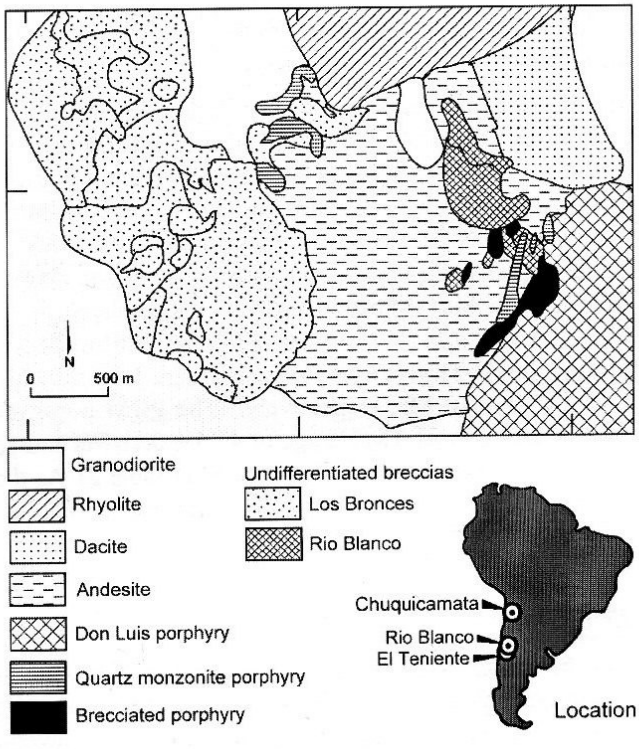

Figure 7: ***Simplified geology of the Rio Blanco area, Chile.*** Inset location plan shows location of Rio Blanco relative to the other deposits discussed, El Teniente and Chuquicamata.

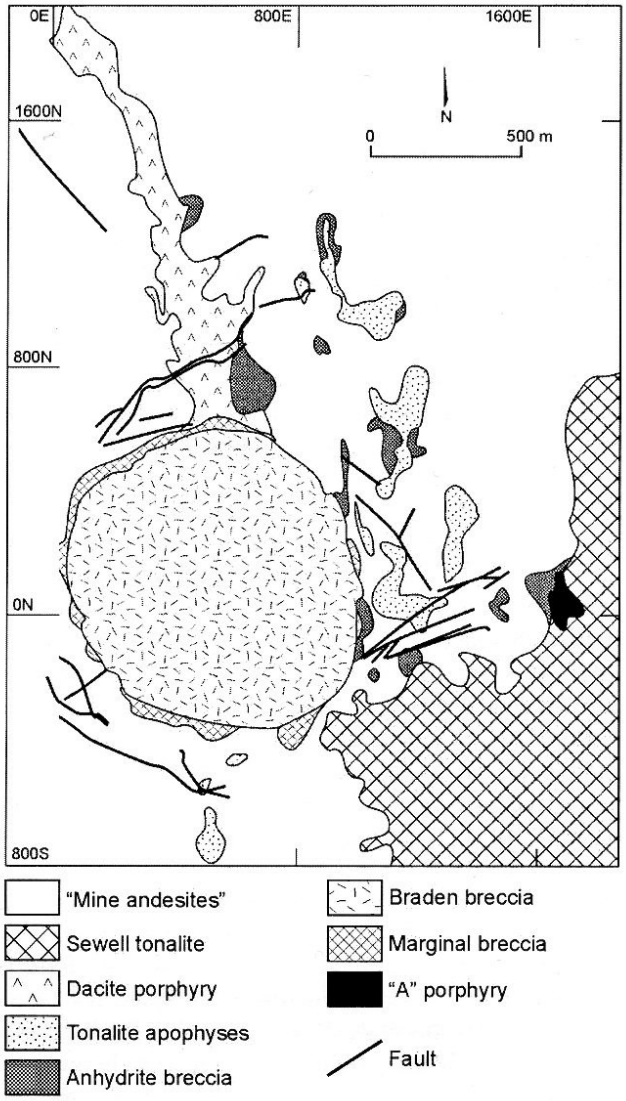

Figure 8: ***Simplified geology of the El Teniente Deposit, Chile,*** Ten-6 level (2165 m). See Fig. 7 for location.

Río Blanco

Río Blanco is a supergiant porphyry Cu-Mo deposit (Fig. 7) located in Central Chile with resources and reserves of 5.100 Mt at 0.79% Cu. Disseminated mineralisation is hosted in a granodiorite unit (Río Blanco) and within a breccia complex, and is thought to be related to the intrusion of the tabular, dyke-like quartz monzonite porphyry (PQM) at 6.32 ± 0.06 Ma (U-Pb) and the Don Luis porphyry (PDL) at 5.23 ± 0.07 Ma (U-Pb) (Deckart *et al.,* 2005). Zircon and apatite (U-Th)/He ages for the PDL are 3.9 ± 0.09 Ma and 2.40 ± 0.10 Ma, respectively. The PQM porphyry yielded a zircon (U-Th)/He age of 4.95 ± 0.18 Ma and an apatite (U-Th)/He age of 3.5 ± 0.14 Ma (Table 2). As the thermal mass at this deposit is dominated by the PDL, we have used the PDL age data and intrusion dimensions for inverse modelling.

El Teniente

The El Teniente Cu-Mo porphyry deposit (Fig. 8) is a supergiant system in Central Chile with resources and reserves of the order of 4424 Mt at 0.9 % Cu. Several stages of molybdenite mineralisation have been identified between 6.4 and 4.2 Ma (Maksaev *et al.,* 2003). The mineralisation is hosted by andesitic volcanics, hydrothermal breccias, felsic porphyries and tonalit intrusives. The late mineralisation event was accompanie by the intrusion of the Teniente Dacite porphyry, whic yielded a zircon U-Pb age of 5.05 ± 0.12 Ma, a molybdeni Re-Os age of 5.14 ± 0.03 Ma and a sericite Ar-Ar age 4.96 ± 0.03 Ma. The latest magmatic record is given b the intrusion of the hornblende rich dykes at 3.94 ± 0.3 Ma (inverse isochron Ar-Ar age). Apatite (U-Th)/He age for the dacite porphyry range from 2.7 to 3.4 Ma.

Discussion and Interpretation

Duration of Hypogene Ore Formation: Measured Modelled

Zircon U-Pb and zircon (U-Th)/He ages of intrusion-relate ore deposits can potentially be used to constrain the duratio of hypogene ore formation because their closur temperatures bracket the magmatic-hydrotherma temperature interval of 750° to 200°C. Taking into accou the age uncertainty estimates, the age differentials indica a maximum period of ore deposition of 3 m.y. for Sa Cheshmeh, 1.4 m.y. for Rio Blanco, and around 0.5 m. for Abdar and Meiduk (Table 2). However, other studie have constrained, through the use of multipl geochronology methods and the age dating of intrusion that cross-cut mineralisation, that intrusion-relate hydrothermal mineralisation takes place within hundre thousand year time frames: Sar Cheshmeh, ~160 K (McInnes *et al.,* 2003); Batu Hijau, ~80 Ka (Garwin, 2002 Grasberg, ~100 Ka (Pollard *et al.,* 2004); Lepanto-Far Soutl East, 100-300 Ka (Arribas *et al.,* 1995); Round Mountain ~100 Ka (Henry *et al.,* 1997). It is probable that thes duration estimates are also maximum values, taking int account the resolution achievable using radiometric datin methods.

The measured geochronology data (Table 2 and Fig. 9) intrusion size estimates and a range of emplacement depth (Table 3) were input into GeoModel v. 1.0 to iteratively reproduce an idealised time-temperature history for eac deposit (Fig. 10). Because the solubility of chalcopyrite the main hypogene ore mineral in porphyry deposits decreases by over two orders of magnitude in hydrotherma fluids during a temperature reduction from 500 to 300°C (McPhail and Liu, 2002; Liu and McPhail, submitted), it i

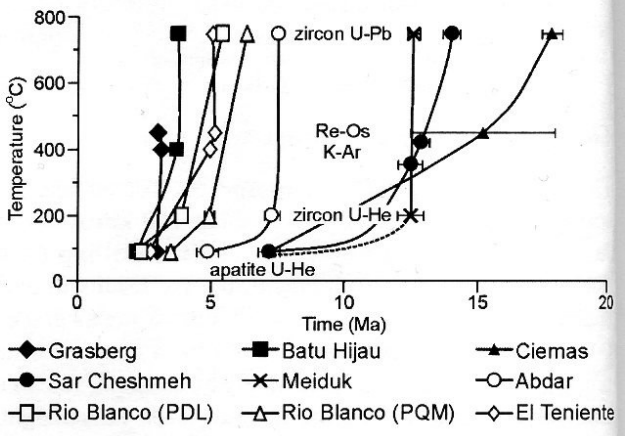

Figure 9: ***Thermal history results as revealed from age data.*** Ages are plotted against closure temperature for the given mineral and dating method. The steepness of the resultant curve is indicative of the rate of cooling of the sample studied.

possible to estimate the duration of hypogene ore formation for each deposit studied by extracting inverse thermal modelling outputs through this temperature interval (Table 3). The modelled ore formation duration results are consistent with intervals previously determined for deposits for which we have comparative data: Sar Cheshmeh - 270 Ka (this study) vs. ~160Ka (McInnes *et al.*, 2003); Batu Hijau - 16 Ka (this study) vs. ~80 Ka (Garwin, 2002); Grasberg - 15 Ka (this study, assuming the zircon U-Pb age is similar to the biotite Ar-Ar age) vs. ~100 Ka (Pollard *et al.*, 2004). Without wishing to put too fine a point on the modelling outputs, those deposits with ore formation durations less than 100 Ka scale are Grasberg, Batu Hijau, El Teniente, Abdar and Meiduk, whereas Sar Cheshmeh and Rio Blanco fall into an intermediate category (100-1000 Ka), and Ciemas shows the longest period of mineralisation potential because it has taken more than 1000 Ka to cool through the 500-300°C interval (Fig. 11).

Emplacement Depth

The main parameters controlling the cooling rate of an intrusion are size, emplacement depth and heat transfer efficiency (conductive vs. advective cooling regime). For similar sized intrusions, deep emplacement and conductive thermal regimes will produce the lowest overall cooling rates whereas shallow emplacement and advective regimes

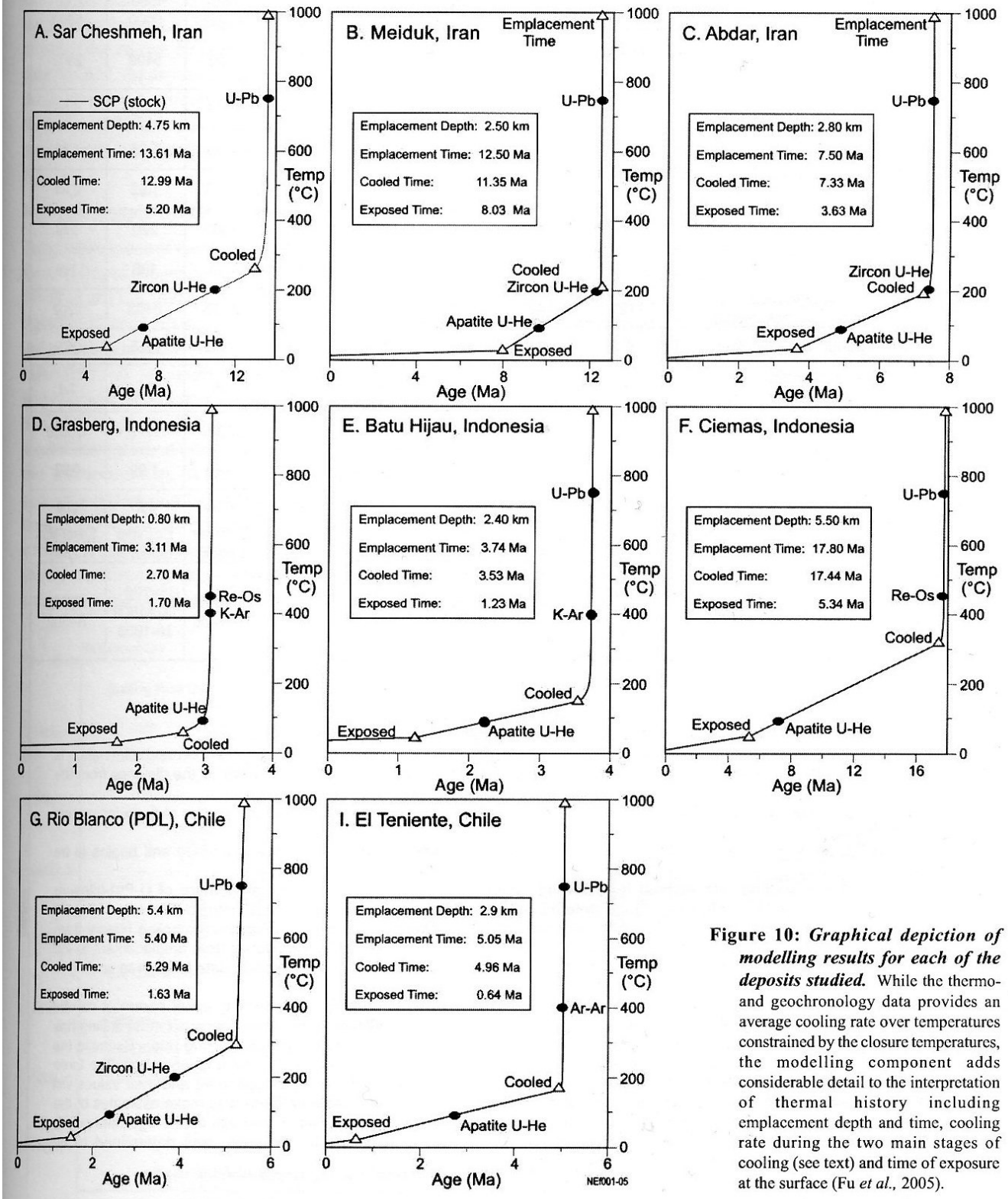

Figure 10: ***Graphical depiction of modelling results for each of the deposits studied.*** While the thermo- and geochronology data provides an average cooling rate over temperatures constrained by the closure temperatures, the modelling component adds considerable detail to the interpretation of thermal history including emplacement depth and time, cooling rate during the two main stages of cooling (see text) and time of exposure at the surface (Fu *et al.*, 2005).

will produce the fastest cooling rates. Raw average cooling rates for the porphyry deposits were calculated (Table 3) based on the age data in Table 2. Of the deposits studied, Grasberg has the fastest (>1000°C/m.y.) and Ciemas the slowest (<100°C/m.y.) raw average cooling rates, with the remaining deposits falling within 100-1000°C/m.y. range (Table 3). Overall average cooling rates calculated by GeoModel v. 1.0 (Table 3) are consistent with the raw results.

As discussed in an earlier section, GeoModel v. 1.0 solv for emplacement depth during cooling in a conducti thermal regime, and therefore the minimum depths emplacement can be determined for intrusions of a giv size. A range of possible emplacement depths along wit best fit model depth are provided in Table 3, and the resul are schematically presented in Fig. 11. The model dep of emplacement for the Iranian porphyry deposits indica that Sar Cheshmeh was emplaced at deeper levels than t

Porphyry Deposit		Kerman Belt, Iran			Indonesia			Chile	
		SCP Sar Cheshmeh	Meiduk	Abdar	Ciemas	Batu Hijau	Grasberg	Rio Blanco (PDL)	El Teniente
Range of Possible Emplacement Depths (m) *		3800-5500	2000-3200	2000-3200	4000-6500	2000-3000	300-1000	4500-6000	2000-5000
Best Fit Emplacement Depth (m) **		4750	2500	2800	5500	2400	800	5400	2900
Age of Emplacement (Ma)		13.61	12.50	7.50	17.80	3.74	3.11	5.40	5.05
Age deposit cooled *** (Ma)		12.99	11.35	7.33	17.40	3.53	2.70	5.29	4.96
Age of Exposure at Surface **** (Ma)		5.20	8.03	3.63	5.34	1.23	1.70	1.63	0.64
Cooling Rate # (°C/My)	Raw Average Cooling Rate from Age Data	103	-	253	62	172	1800	220	279
	Modelled Overall Average	73.5	80.0	133	56.2	267	321	185	198
	Magmatic - HydrothermalCooling	1121	742	4721	1890	4295	2190	6108	9202
	Exhumation Cooling	23.5	13.0	26.9	18.3	43	29.8	58.5	35.9
300~500 °C Interval	Duration (K.y.)	270	10.0	6.5	1040	10.5	15	101.4	1.6
	Cooling Rate(°C/M.y.)	741	20000	30769	192	18868	13333	1972	125000
Average Exhumation Rate (km/M.y.)		0.39	0.26	0.43	0.35	0.72	0.38	1.09	0.62
Porphyry eroded since exposure (m)		312	800	435	587	300	408	490	250
Modelling Parameters	Shape	Cylinder (stock)	Ellipsoid (stock)	Cylinder (stock)	Cylinder (stock)	Cylinder (stock)	Cylinder (stock)	Ellipsoid (sphere)	Sheet-like (dyke)
	Dimension (m) of Deposit ##	D1=2200 D2=1000 H=1000	D1=400 D2=700 H=700	D=750 H=900	D=1000 H=1000	D=500 H=1700	D=950 H=1700	D1=700 D2=1800 H=1000	W=150 H=800

Assumptions and Notes

Constant surface temperature = 10.0 °C; Constant heat flow from bottom = 65 mW/m°C
Thermal gradient = 50.0 °C/Km (Abdar: 60°C/Km); Initial temperature = 1000 °C; Diffusivity = 10^{-6} m^2/s.

* Range of possible valid values for emplacement depth (m) for each intrusion. A process of iteration and elimination is used to find the best fit value (see Appendix I). ** Emplacement depth is defined in the model as the distance from the palaeosurface to the top of the igneous body.

*** The igneous body has "cooled" when it reaches the same temperature as the surrounding country rock under normal geothermal gradient conditions.

**** Age of Exposure is defined as the time when the top of the igneous body is exposed at surface and begins to be eroded.

The raw average cooling rate derived from the age data is calculated as ((closure temperature of U-Pb)-(closure temperature of apatite (U-Th)/He)) / ((age determined by U-Pb) – (age determined by apatite (U-Th)/He)). "Overall Average" cooling rate refers to the cooling rate calculated by GeoModel v.1 over the complete cooling history from 1000°C to surface temperature of 10°C. Magmatic-hydrothermal cooling refers to the cooling from emplacement to the "cooled" state as defined above. Exhumation cooling refers to the interval from the "cooled" state through to cooling to surface temperature of 10°C.

##D = stock diameter, W = dyke width. Although the horizontal dimension of an igneous body is either known or can be closely estimated from geological evidence, its height (H) is often very difficult to determine because most drilling has only partially penetrated the ore body. Extension of the intrusion at depth would decrease cooling rate. Because the height is often poorly constrained, the emplacement depth, eroded thickness and height of the igneous body are three variables that have to be assumed for each run of the model. These variables are independent and their values will affect the cooling history of the sample. The current solution to this three-variable problem is to make estimates of the variables and then iterate the calculation until the model produces a curve that passes through all the age data points (see Appendix I). Using this method, the erosion rate at Sar Cheshmeh, for example, was determined to be 0.06 mm/yr.

Table 3: ***Summary of inverse thermal modeling results using GeoModel 1.0***

Meiduk and Abdar intrusions (Table 3, Fig. 11). Geological reconstruction of the Kuh-e-Masahim volcano indicates that approximately 2 km of volcanic cover overlying the Abdar intrusion has been eroded (McInnes, unpublished data), consistent with the minimum possible emplacement depth generated by the model (Table 3). Similarly in Indonesia, model depths of emplacement for Grasberg of 800 m are supported by independently determined geological data that the Main Grasberg Intrusion was emplaced into a volcanic edifice within 1 km of the palaeosurface (MacDonald and Arnold, 1994; Weiland and Cloos, 1996). At Batu Hijau, the modelled depth of emplacement of 2400 m (-400/+600 m) is consistent with palaeodepth reconstruction by Garwin (2002) of 2000 ± 500 m. The depth estimate for the Ciemas deposit is 5500 m below the palaeosurface, although this cannot be corroborated by other geological data. In Chile, the depth of emplacement of the El Teniente dacite porphyry is estimated to be around 2900 m whereas the PDL and PQM intrusion samples from the Rio Blanco deposit were emplaced at a depth of 5400 m (Table 3, Fig. 11).

Hypogene Copper Grade as a Function of Cooling Rate

Temperature is one of the fundamental variables controlling the solubility of copper in magmatic-hydrothermal systems (McPhail and Liu, 2002; Liu and McPhail, submitted) and therefore thermal history analysis may prove useful in understanding processes that produce high-grade hypogene ores. One way to rapidly deposit Cu-sulphide minerals within small rock volumes is to pass a hydrothermal fluid through a steeply declining thermal gradient. In contrast, weak thermal gradients should generate more diffuse haloes of Cu mineralisation. A schematic representation of this concept is provided in Fig. 1 where Cu transport and heat transfer are treated as diffusive processes. Under these conditions, intrusions emplaced within the uppermost crust should experience greater thermal gradients than those emplaced in mid-crustal regions where temperature regimes are moderated by the Earth's geotherm. Support for the cooling rate hypothesis can be found in the Indonesian study set (Fig. 11). Grasberg, the most shallowly emplaced intrusion-related hydrothermal system with a high average Cu grade of 1.08% experienced the highest rate of cooling of any porphyry system studied. In contrast, the Ciemas porphyry with an average grade of 0.2% Cu has the slowest cooling rate over the hypogene temperature interval (almost 200°C/m.y.) and is interpreted to be the most deeply emplaced intrusion (5.5km). It took over 1 m.y. for Ciemas to cool through the hypogene Cu window, and it is possible that the low Cu grades for the deposit might be explained by the fact that the original magmatic Cu was distributed over a larger volume of country rock. It is suggested therefore that in the Indonesian examples, Grasberg experienced the thermal gradient conditions of the pluton depicted in the right of Fig. 1 and Ciemas represents the pluton on the left. This is also supported by their contrasting "hockey stick" patterns shown in Fig. 9.

Thermal history analysis of the Rio Blanco deposit (average grade of 0.79% Cu) indicates that it was emplaced at almost the same depth as Ciemas, yet Rio Blanco cooled ten times faster through the hypogene Cu window. This example points out that emplacement depth is not the only controlling factor and that advective heat transfer processes also need to be considered. The permeable breccia formations at Rio Blanco may have provided a more efficient heat transfer mechanism than that which existed during the cooling of the Ciemas magmatic-hydrothermal system and this might explain why the Cu grade is relatively higher at Rio Blanco. Although this preliminary study suggests a correlation might exist between cooling rate and hypogene copper grade in porphyry Cu deposits, it is not know whether thermal history analysis can be applied to mineral exploration. Other factors such as total metal availability reactivity of wall rock (e.g., carbonates at Grasberg) and periodic pulses of metal emplacement cannot be assessed

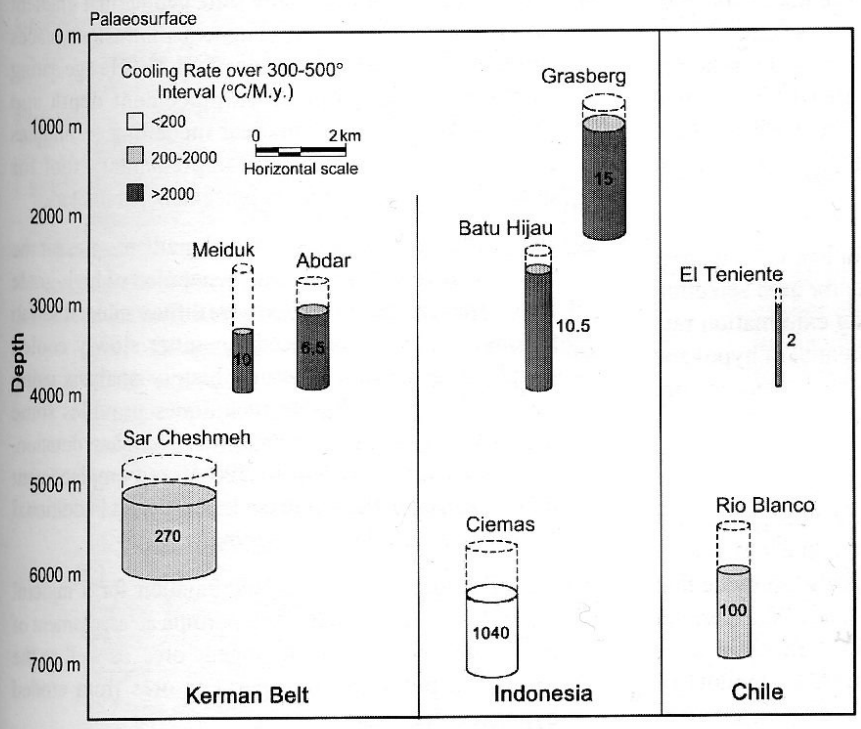

Figure 11: ***Schematic representation of emplacement depth as determined by GeoModel.*** Intrusion diameters are those used in the model (Table 3) and all intrusions are modelled at 1000 m high. Dotted cylinder represents the amount of material eroded from each intrusion since exposure at surface (Table 3). Numbers inside cylinders represent the modelled duration of the 300-500°C cooling interval for each intrusion (Ky). The higher the cooling rate over this same temperature interval, the darker the shading of the cylinder.

through thermal history analysis. More studies of intrusions on a regional scale are needed to increase the data density and definitively assess the relationships between cooling rate and hypogene Cu grade.

Preservation Potential of Hypogene Ores and Potential Formation of Supergene Ores

As discussed earlier, GeoModel v. 1.0 treats the cooling of intrusive bodies from magmatic temperatures to surface temperatures (in this study nominated as 10°C) as a two-stage process: i) magmatic-hydrothermal cooling (R_1 in Fig. 1) and ii) exhumation cooling (R_2 in Fig. 2). Exhumation cooling is controlled by the rate of removal of cover material overlying the sample by tectonic (e.g., extension) and/or erosional processes (e.g., glaciation). If a post-emplacement exhumation rate can be determined for an intrusion, then an assessment of the preservation potential of associated hypogene mineralisation can be made. Exhumation rates for the porphyry deposits studied range from 0.3 to 1.1 km/m.y. (Table 3). The highest overall exhumation rates were for Rio Blanco (1.1 km/m.y.) and El Teniente (0.6 km/m.y.) consistent with their occurrence in glaciated alpine terranes undergoing relatively rapid uplift. Grasberg, in a similar orogenic and climatic setting has a lower calculated exhumation rate of 0.38 km/m.y.. Other workers (Weiland and Cloos, 1996; Hill *et al.*, 2002) have argued that although rapid denudation (0.7-1.0 km/m.y.) is occurring along major thrust fronts actively forming the New Guinea Fold Belt, these fronts are 50 km distant from the Grasberg deposit and that the peak uplift forces have not yet transitioned to the Grasberg area. The other deposit with relatively high exhumation rates is Batu Hijau (0.72 km/m.y.), where a combination of collision-driven Pliocene uplift (Garwin, 2002 and references therein) and pluvial processes were occurring. Collision-driven uplift is also a feature of the Kerman Belt where the majority of uplift is occurring along the actively deforming Zagros Thrust Zone. The exhumation rates determined for the Sar Cheshmeh, Meiduk and Abdar deposits are within a narrow range of 0.3-0.4 km/m.y., presumably because they are located co-parallel and 80 km distant from the Zagros Thrust Zone.

Understanding the rate of exhumation for a mineral district or a metallogenic belts has implications for area selection during mineral exploration. Quantifying exhumation rate permits an assessment of the erosion potential of hypogene ores and an evaluation of the potential for supergene ore formation from eroded hypogene deposits. Fig. 11 portrays the amount of erosion experienced by each intrusion as a dashed cylinder. In Indonesia, Batu Hijau has experienced the least amount of erosion since exposure whereas Ciemas has experienced the most. In Chile, the thickness of eroded porphyry mineralisation at Rio Blanco is almost twice that eroded at El Teniente. Although the deposits of the Kerman belt have similar exhumation rates, differences in their exposure age indicate substantially different amounts of potential hypogene mineralisation have been eroded.

Taking Sar Cheshmeh as an example, the porphyry copper deposit was exposed 5.2 million years ago and was exhumed at a rate of 0.39 km/m.y. (Table 3), while the erosion rate for the porphyry since exposure is estimated to be about 0.06 km/m.y. (see notes, Table 3). These calculations infer that 312 m of porphyry Cu mineralisation has eroded since exposure of the porphyry at surface. Assuming an average copper shell thickness of 100 m and a rock density of 2.7 g/cm^3, the total amount of rock eroded from the Sar Cheshmeh porphyry system was about 81 million tonnes (Mt). The Sar Cheshmeh porphyry was intruded by three copper-poor igneous dyke units that account for about 1/3 of the deposit volume, so the total amount of eroded ore is reduced to 540 Mt. At a minimum copper grade of 0.64%, the total amount of copper eroded equates to around 3.5 Mt, which is nearly half of the remaining reserve as estimated in 1998. If the amount of supergene Cu contained at Sar Cheshmeh is less than the amount of Cu contained in the material eroded, then the unaccounted Cu may be contained in Exotica-type deposits below sedimentary and volcanic cover in the region. This assumes the rate of uplift and erosion did not outstrip the rate of weathering and leaching since the deposit was first exposed. Similar calculations can be performed for the other deposits to assess both the preservation potential of hypogene shells and the potential for formation of supergene ore deposits.

Conclusions

i) Combining apatite (U-Th)/He, zircon (U-Th)/He and zircon U-Pb ages provides a thermal history for porphyry deposits over a temperature range of >700°C. Information that can be obtained from thermal history analysis includes the timing and depth of emplacement of igneous units, the cooling rate during hypogene copper deposition and the exhumation rate of the porphyry deposit.

ii) The disruption of the steady state geothermal gradient during the emplacement of igneous intrusions places limitations on the direct usage of (U-Th)/He age dating in the determination of emplacement depth and exhumation rates. Numerical modelling techniques provide an effective and complementary tool for quantifying cooling and emplacement parameters.

iii) We postulate that strong thermal gradients present the most ideal conditions for the generation of high-grade hypogene Cu ores, whereas more diffuse mineralisation haloes would be expected for more slowly cooled porphyry systems. Thermal history analysis using "triple dating" U-Pb-He techniques provides some support for a positive correlation between short duration, rapid cooling from 500 to 500°C and emplacement depth, however the database is limited and additional district-scale studies are required.

iv) Understanding the rate of exhumation for a mineral district or a metallogenic belt permits an assessment of the erosion potential of hypogene ores, as well as the formation potential of supergene ores from eroded hypogene deposits.

Acknowledgements

The management of NICICO is gratefully acknowledged for providing access to Sar Cheshmeh, Meiduk and Abdar. Thanks to Jeff Davis and Ahmed Ali for mineral separations, Ratih Woodhouse and Marcus Gregson for hand-picking/ quality control, Lesley Dotter for zircon dissolutions, Peter Pollard for provision of the Grasberg geology image, Travis Naughton for drafting, and Esmail Heidari and Hussein Taghizadeh for help in the field. We are grateful to Rio Tinto Mining and Exploration Ltd, in particular Neil McLaurin and John Bartram, for supporting this work and permitting its publication. Field and laboratory activities in Indonesia were supported by a GRDC Capacity Building Program supported by AusAID, CSIRO, and the Indonesian Department of Energy and Mineral Resources. This is contribution 405 from the GEMOC ARC National Key Centre (www.els.mq.edu.au/GEMOC).

References

Arehart, G.B., Chakurian, A.M., Tretbar, D.R., Christensen, J.N., McInnes, B.I.A. and Donelick, R.A., 2003 - Evaluation of radioisotope dating of Carlin-type deposits in the Great Basin, Western North America, and implications for deposit genesis; *Economic Geology,* v. 98, pp. 235-248.

Arribas, A. Jr., Hedenquist, J.W., Itaya, T., Okada, T., Concepcion, R.A. and Garcia, J.S. Jr., 1995 - Contemporaneous formation of adjacent porphyry and epithermal Cu-Au deposits over 300 Ka in northern Luzon, Philippines; *Geology,* v. 23, pp. 337-340.

Ballard, J.R., Palin, J.M., Williams, I.S., Campbell, I.H. and Faunes, A., 2001 - Two ages of phorphyry intrusion resolved for the super-giant Chuquicamata copper deposit of northern Chile by ELA-ICP-MS and SHRIMP; *Geology,* v. 29, pp. 383-86.

Cartwright, T., 1998 - Petrology report on 22 samples from Ciemas, West Java for Meekatharra Minerals; *Kinston Morrison Mineral Services,* 38p.

Cherniak, D.J. and Watson, E.B., 2000 - Pb diffusion in zircon; *Chemical Geology,* v. 172, pp. 5-24.

Crowhurst, P.V.C., Farley, K.A., Ryan, C., Duddy, I. and Blacklock, K., 2002 - Potential of rutile as a (U-Th)-He thermochronometer; *Geochimica Cosmochimica Acta,* v. 66, p. A-158.

Deckart, K., Clark, A.H., Aguilar, C.A. and Vargas, R.R., 2005 - Magmatic and hydrothermal chronology of the supergiant Rio Blanco porphyry copper deposit, Central Chile: Implications of an integrated U-Pb and $^{40}Ar/^{39}Ar$ database; Accepted by *Economic Geology*; Special issue on "Giant Porphyry Cu-Mo deposits of the Andean and PNG/ Irian Jaya foldbelts".

Evans, N.J., Wilson, N.S.F., Cline, J.S., McInnes, B.I.A., Farley, K.A. and Byrne, J., 2005 - (U-Th)/He Thermochronology of Fluorite and the Low Temperature History of Yucca Mountain, Nevada; In press, *Applied Geochemistry.*

Farley, K.A., 2002 - U-He dating: Techniques, calibrations and applications; *in* Noble Gases in Geochemistry and Cosmochemistry; *Reviews in Mineralogy and Geochemistry,* v. 47, pp. 819-844.

Fu, F.Q., McInnes, B.I.A., Davies, P.J. and Evans, N.J., 2005 - Numerical modeling of the thermal and exhumation histories of ore systems as constrained by (U-Th)/He thermochronometry and U-Pb dating; Submitted to *Economic Geology.*

Garwin, S.L., 2000 - The setting, geometry and timing of intrusion-related hydrothermal systems in the vicinity of the Batu Hijau porphyry copper-gold deposit, Sumbawa, Indonesia; Unpublished Ph.D. dissertation, *University of Western Australia,* Nedlands, 320p.

Garwin, S., 2002 - The geologic setting of intrusion-related hydrothermal systems near the Batu Hijau porphyry copper-gold deposit, Sumbawa, Indonesia, *in* Goldfarb, R.J. and Nielsen, R.L. (Eds.), Integrated Methods for Discovery: Global Exploration in the 21st Century; *Society of Economic Geologists,* Special Publication 9, pp. 333-366.

Ghorashi-Zadeh, M., 1979 - Development of hypogene and supergene alteration and copper mineralisation patterns, Sar Cheshmeh porphyry copper deposit, Iran; Unpublished M.Sc. Thesis, *Brock University,* 223p.

Hassanzadeh, J., 1993 - Metallogenic and tectonomagmatic events in the SE sector of the Cenozoic active continental margin of central Iran (Shahr e Babak area, Kerman Province); Unpublished Ph.D. Thesis, *UCLA,* 204p.

Henry, C.D., Elson, H.B., McIntosh, W.C., Heizler, M.T. and Castor, S.B., 1997 - Brief duration of hydrothermal activity at Round Mountain, Nevada, determined from $^{40}Ar/^{39}Ar$ geochronology; *Economic Geology,* v. 92, pp. 807-826.

Jackson, S.E., Pearson, N.J., Griffin, W.L. and Belousova, E.A., 2004 - The application of laser ablation-inductivevly coupled plasma-mass spectrometry to *in-situ* (U-Th)/He-Pb zircon geochronology; *Chemical Geology,* v. 211, pp. 47-69.

Lee, J.K.W., Williams, I.S. and Ellis, D.J., 1997 - Pb, U and Th diffusion in natural zircon; *Nature,* v. 390, pp. 159-162.

Liu, W. and McPhail, D.C., Thermodynamic properties of copper chloride complexes and copper transport in magmatic hydrothermal solutions; Submitted to *Chemical Geology.*

Maksaev, V., Munizaga, F., McWilliams, M., Mathur, R., Ruiz, J., Fanning, M.C. and Zentilli, M., 2003 - New Timeframe for El Teniente Cu-Mo Giant Porphyry Deposit: U-Pb, $^{40}Ar/^{39}Ar$, Re-Os and Fission Track Dating. *Short Papers - IV South American Symposium on Isotope Geology,* IV SSAGI, August 24th - 27th, 2003, [CD-ROM], Salvador, Bahia, Brazil, pp. 736-739.

Mathur, R., Ruiz, J. and Munizaga, F., 2000a - Relationship between copper tonnage of Chilean base metal

porphyry deposits and Os isotope ratios; *Geology,* v. 28, pp. 555-558.

Mathur, R., Ruiz, J., Titley, S., Gibbons, S. and Margotomo, W., 2000b - Different crustal sources for Au-rich and Au-poor ores of the Grasberg Cu-Au porphyry deposit; *Earth and Planetary Science Letters,* v. 183, pp. 7-14.

McDougall, I. and Harrison, M.T., 1999 - Geochronology and Thermochronology by the $^{40}Ar/^{39}Ar$ Method; 2nd edition, *Oxford University Press,* 269p.

McDowell, F.W., McMahon, T.P., Warren, P.Q. and Cloos, M., 1996 - Pliocene Cu-Au bearing intrusions of the Gunung Bihj (Ertsberg) district, Irian Jaya, Indonesia: K-Ar geochronology; *Journal of Geology,* v. 104, pp. 327-340.

McInnes, B.I.A., Farley, K.A., Sillitoe, R.H. and Kohn, B.P., 1999 - Application of apatite U-He thermochronometry to the determination of the sense and amount of vertical fault displacement at the Chuquicamata porphyry copper deposit, Chile; *Economic Geology,* v. 94, pp. 937-945.

McInnes, B.I.A., Evans, N.J., McBride, J., Keays, R. and Lambert, D., 2000 - Metallogenic fertility and Re-Os geochronology of ore systems; *CSIRO Exploration and Mining* Confidential Report 921C. 41p.

McInnes, B.I.A., Evans, N.J., Sukarna, D., Permanadewi, S., Garwin, S., Belousova, E., Griffin, W.L. and Fu, F.Q., 2004 - Thermal histories of Indonesian porphyry Cu-Au deposits determined by U-Pb-He and K-Ar methods; *in* Muhling, J., Goldfarb, R., Vielreicher, N., Bierlein, F., Stumpff, E., Groves, D.I. and Kenworthy, S., (Eds), Predictive Mineral Discovery Under Cover: Extended Abstracts; *Centre for Global Metallogeny, The University of Western Australia,* Publication 33, pp. 343-346.

McPhail, D.C. and Liu, W., 2002 - Metal transport in hypersaline brines; *Geological Society Australia* Abstracts, v. 67, p. 295.

Pollard, P.J., Taylor, R.G. and Peters, L., 2004 - Ages of intrusion, alteration and mineralization at the Grasberg Cu-Au deposit, Irain Jaya, Indonesia; Submitted to *Economic Geology,* Special issue on Giant Porphyry Cu Deposits.

Reiners, P.W., Farley, K.A. and Hickes, H.J., 2002 - He diffusion and U-He thermochronometry of zircon: Initial results from Fish Canyon Tuff and Gold Butte; *Tectonophysics,* v. 349, pp. 297-308.

Reynolds, P., Ravenhurst, C., Zentilli, M. and Lindsay, D., 1998 - High-precision $^{40}Ar/^{39}Ar$ dating of two consecutive hydrothermal events in the Chuquicamata porphyry copper system, Chile; *Chemical Geology,* v. 148, pp. 45-60.

Sengor, A.M.C. and Kidd, W.S.F., 1979 - Post-collisional tectonics of the Turkish-Iranian plateau and a comparison with Tibet; *Tectonophysics,* v. 55, pp. 361–376.

Shahabpour, J., 1982 - Aspects of alteration and mineralization at the Sar-Cheshmeh copper-molybdenum deposit, Kerman, Iran; Unpublished Ph.D. Thesis, *University of Leeds,* 342p.

Suzuki, K., Shimizu, H. and Masuada, A., 1996 - Re-O dating of molybdenites from ore deposits in Japan Implication for the closure temperature of the Re Os system for molybdenite and the cooling histor of molybdenum in ore deposits; *Geochimic Cosmochimica Acta,* v. 60, pp. 3151-3159.

Waterman, G.C. and Hamilton, R.L., 1975 - The Sa Cheshmeh porphyry copper deposit; *Economi Geology,* v. 70, pp. 568-576.

Weiland, R.J. and Cloos, M., 1996 - Pliocene-Pleistocen asymmetric unroofing of the Irian fold belt, Iria Jaya, Indonesia: apatite fission-trac thermochronology; *Geological Society of Americ* Bulletin, v. 108, pp. 1438-1449.

Zeitler, P.K., Herczeg, A.L., McDougall, I. and Honda, M 1987 - U-Th-He dating of apatite: A potenti thermochronometer; *Geochimica Cosmochimic Acta.,* v. 51, pp. 2865-2868.

Appendix I. Explanation of Model Parameters

Sample Position, Eroded Thickness of the causal intrusion, and Initial Sample Depth

A software package, GeoModel v. 1.0, has been developed to conduct inverse thermal modelling of U-Pb-He age data (Fu *et al.*, 2005). In order to run the algorithm, the sample position within the intrusion must be either known or assumed. As shown in Fig. 12, the distance from the "top" of the intrusion to the sample position at the Present Surface is defined as the "Eroded Thickness".

If the sample was collected from the Present Surface, then the position of the sample at the time of emplacement, termed the Initial Sample Depth, is defined as the:

Emplacement Depth + Eroded Thickness

If samples are taken from drill holes, then the Initial Sample Depth

= Emplacement Depth + Eroded Thickness + vertical distance below Present Surface.

Calculation of Emplacement Depth

Determination of emplacement depth and calculation of erosion rates is based on the assumption that erosion processes have occurred continuously at the surface since the time of intrusion. For each run of the model, we assign initial values for the Emplacement Depth and Eroded Thickness of the intrusion and then calculate a cooling curve for the sample. If this cooling curve passes through all of the measured age data points, then this run of the model is considered to be successful, and the Emplacement Depth and Eroded Thickness are "possible" valid values. The word "possible" is used here because there are a number of other pairs of Emplacement Depth and Eroded Thickness values that can also satisfy the model and result in successful cases. This introduces some uncertainty in the final result. Fortunately, the Emplacement Depth can be limited to a certain range. Beyond this range, no matter what value of Eroded Thickness is taken, the model will fail. Similarly, the Eroded Thickness can be limited to a narrow range.

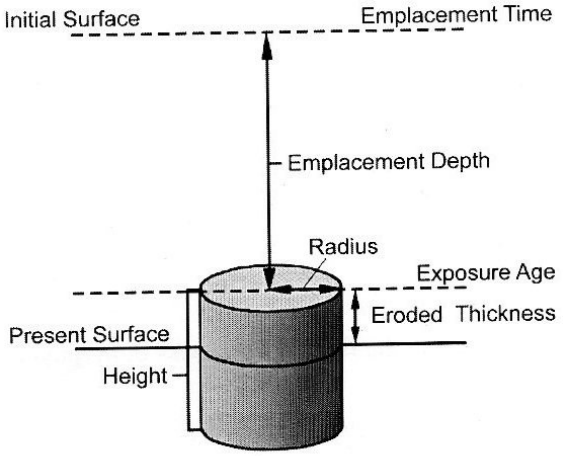

Figure 12. ***Terminology of inverse thermal modeling of cylindrical intrusions in GeoModel v 1.0*** (Fu *et al.*, 2005)

Calculation of Exhumation Rate

The apatite (U-Th)/He age was used to calculate a depth (called He Depth) which corresponds to the position of the sample at the time of closure for apatite (U-Th)/He. For example, if we assume the apatite (U-Th)/He age is 1 Ma with a closure temperature = 90°C (based on a cooling rate of 100°C/m.y.), a surface temperature = 10 °C, and a thermal gradient = 50°C/km, then the depth of the sample at 1 Ma:

He Depth = (90-10) / 50 = 1.6 km

So, we can say, under the above conditions, that the sample was at a depth of 1.6 km below the surface 1 m.y. ago.

The erosion rate (Rate 1), before exposure is defined as:

$$\text{Rate 1} = \frac{\text{Initial Sample Depth} - \text{He Depth}}{\text{Emplacement Time} - \text{He Age}} \quad \text{..... Equation 1}$$

The erosion rate (Rate 2), after exposure of the intrusion is defined as:

$$\text{Rate 2} = \frac{\text{Eroded Thickness}}{\text{Exposure Age}} \quad \text{..... Equation 2}$$

Where the Eroded Thickness of Intrusion

= Initial Sample Depth – Rate 1 x [Emplacement Time – Exposure Age]

The Exposure Age will be generated automatically by the model when the top of the intrusion is exposed and begins to erode.

The calculation of He Depth is based on the assumption that the intrusion is already "cooled" (as defined in Table 3 and the text) before it passes through the closure temperature of apatite (U-Th)/He. Most deposits in this study fall into this category. If it is not "cooled" (like Grasberg), the calculation is more complicated but follows the same general assumptions outlined above.

Example: Determination of emplacement depth and exhumation rate for the Batu Hijau porphyry system

Thermochronometry	Closure temp	Age (Ma)	Note
Apatite (U-Th)/He	90°C	2.23 ± 0.09	He Depth = 1600 m
K-Ar	400°C	3.73 ± 0.08	
U-Pb	750°C	3.74 ± 0.14	Emplacement time=3.74 Ma

Batu Hijau was modelled as a cylindrical stock with a diameter of 500 m and height of 1700 m. Theoretical modellin studies show that igneous bodies 500 m wide and about 2000 m high would be "cooled" within <1 m.y. if the Emplacemer Depth was <10 km. So the Batu Hijau porphyry would have "cooled" before it reached the apatite (U-Th)/He closu temperature (90°C).

We can constrain the valid range of Emplacement Depth for Batu Hijau before running the model. For example:

i) If Emplacement Depth = 2.6 km and Eroded Thickness of porphyry = 0m, the erosion rate before exposure is abo 0.66 mm/yr using Equation 1.

   Rate 1 = (2.6 km - 1.6 km) / (3.74 Ma - 2.23 Ma) = 1.0km / 1.51m.y. = 0.66225 km/m.y. (or mm/yr)

   At this rate, Batu Hijau would still not be exposed because the eroded thickness of country rock would be 2.48 k (0.66225 km/m.y. * 3.74 m.y.), less that the emplacement depth (2.6 km). Therefore, the emplacement depth must b deeper than 2.6 km.

ii) If we assume the Eroded Thickness of the porphyry is 0~1000m, the <u>minimum</u> Emplacement Depth for Batu Hijau 2.2 ~ 2.6 km;

iii) If Emplacement Depth = 3.5 km and Eroded Thickness of porphyry = 0m, the model will generate an erosion ra before exposure of about 1.33 mm/yr and an erosion rate after exposure of about 0.003 mm/yr. The exposure tim would be 1.05Ma. This is an unlikely scenario so the Emplacement Depth must be less than 3.5 km.

iv) If we assume the Eroded Thickness of porphyry is 0~1000 m, the <u>maximum</u> Emplacement Depth for Batu Hijau is 3.0-3.4 km;

v) Once the Emplacement Depth is constrained, we can also constrain the Eroded Thickness of the intrusion by considerin the erosion rate of the overlying country rock and porphyry rock units.

Then, based on the ranges of Emplacement Depth and Eroded Thickness obtained, we can generate a cooling curve th matches all the measured age data and produces reasonable erosion rates. An Emplacement Depth of 2.8 km and Erode Thickness of about 160 m are geologically reasonable and produce a cooling curve that successfully passes through all ag data points (Fig. 9e). The calculated average erosion rate for the Batu Hijau porphyry is 0.26 mm/yr, a value consisten with erosion rates calculated for other porphyry units in the region (e.g., Grasberg = 0.24 mm/yr and Ciemas = 0.15 mm/yr).